ACS OMEGA

Open Access

http://pubs.acs.org/journal/acsodf

Article

Inhibition of MIF with an Allosteric Inhibitor Triggers Cell Cycle Arrest in Acute Myeloid Leukemia

Georgios Pantouris,* Leepakshi Khurana, Pathricia Tilstam, Alison Benner, Thomas Yoonsang Cho, Martin Lelaidier, Mathieu Perrée, Zoe Rosenbaum, Lin Leng, Francine Foss, Vineet Bhandari, Amit Verma, Richard Bucala, and Elias J. Lolis*

Cite This: *ACS Omega* 2025, 10, 17441−17452

Read Online

ACCESS | Metrics & More | Article Recommendations | Supporting Information

ABSTRACT: Macrophage migration inhibitory factor (MIF) is a key modulator of innate and adaptive immunity that has been extensively reported to promote tumor cell survival, proliferation, and metastasis. A recent study focusing on the microenvironment of acute myeloid leukemia (AML) showed that pharmacological inhibition of MIF signaling, *in vitro* as well as *in vivo*, reduces AML cell survival. Such data highlights the crucial role of MIF in AML pathogenesis and support the efforts for developing selective MIF modulators. Here, we report the identification and crystallographic characterization of a MIF inhibitor (compound **1**) with an allosteric binding motif. Single point screening of **1** against a panel of National Cancer Institute (NCI) 60 human tumor cell lines revealed a selective antitumor activity for the AML cell line HL-60. After confirming the protein's expression in multiple AML cell lines, we utilized **1** to extract mechanistic insights into MIF action. Our findings demonstrate that AML cells utilize an MIF-dependent proliferation mechanism, which upon inhibition triggers a G0/G1 cell cycle arrest of the malignant cells. Complementary analysis of the MIF receptors utilizing neutralizing antibodies and selective small molecule antagonists associates this effect with inhibition of CD74 activation. The collection of data presented herein highlights the important role of MIF in proliferation of AML cells and points to the need of developing small molecule anticancer therapeutics that target MIF signaling.

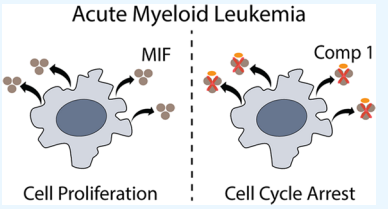

INTRODUCTION

AML is an aggressive hematological cancer[1,2] with multiple types that are defined according to the differentiation markers and criteria reported in the fifth edition of the World Health Organization Classification of Hematolymphoid Tumors.[3] These heterogeneous groups of cells are the result of chromosomal translocations, mutations, upregulation or down-regulation of protein expression, and dysfunction in various signaling pathways. Technological advances including next-generation sequencing have led to personalized treatments, which increased the overall lifespan of AML patients. Nevertheless, relapse remains the most challenging aspect in AML. Conventional treatment plans involve multiple cycles of anthracyclines/cytarabine via intravenous injection, which is well tolerated in AML patients under the age of 60.[3] In older patients though, the success rate of this intense chemotherapeutic regimen is discouragingly low, resulting in a 5-year survival of less than 10−15%.[4] Therefore, the discovery of new therapeutic approaches that are more effective and less toxic is necessary.[5]

Depending on the cell type, release of MIF has autocrine and paracrine effects that promote cell growth and survival.[6,7] In solid cancers such as lung, prostate, cervical, hepatocellular, and renal carcinomas, the activity of MIF is also responsible for malignant cell migration, angiogenesis, and metastasis.[8] Whereas in AML, the role of MIF in cell migration and metastasis is not fully understood, active research on this subject is currently ongoing. In AML blasts of the bone marrow, hypoxia-inducible factor 1-α (HIF-1α) is known to induce the expression of MIF at a higher rate compared to peripheral blood.[9] The knockdown of MIF by lentivirus, *in vitro* and *in vivo*, reduced survival of primary AML, pointing out that MIF would potentially serve as a molecular target for this malignancy. A recent study focusing on the microenvironment of AML showed that secretion of MIF by bone marrow macrophages plays a key role in the survival of AML blast.[10] MIF activity is primarily associated with activation of the type II receptor CD74, which has CD44 as a signaling coreceptor.[11] Notably, single-cell technology, *in vitro*, and *in vivo* experiments identified CD44 and CD74 in AML and showed that they are associated with poor survival.[12−14]

Besides the central cytokine activity, MIF also serves as a noncognate ligand of CXC chemokine receptors, CXCR2 and CXCR4,[15] has a nuclease activity,[16] and functions as an enzyme catalyzing keto/enol tautomerization reactions.[17] The

Received: December 3, 2024
Revised: February 16, 2025
Accepted: February 21, 2025
Published: April 22, 2025

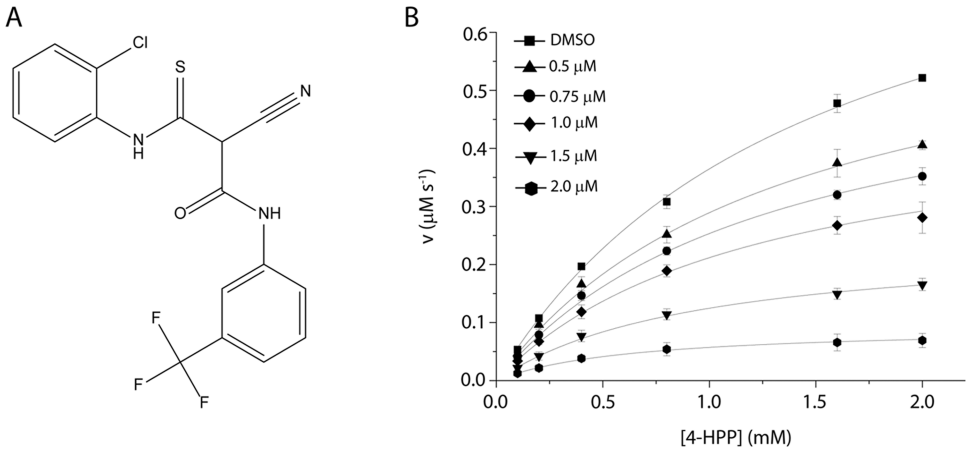

Figure 1. Identification of **1** as a micromolar inhibitor of MIF. (A) Chemical structure of **1**. (B) Michaelis−Menten plot of MIF in the presence or absence of **1**. The inhibition potency of the compound was examined by the 4-HPP keto/enol tautomerase assay at a concentration range of 0−2 mM. Kinetic assays were repeated in triplicate and the error is shown as ± SD.

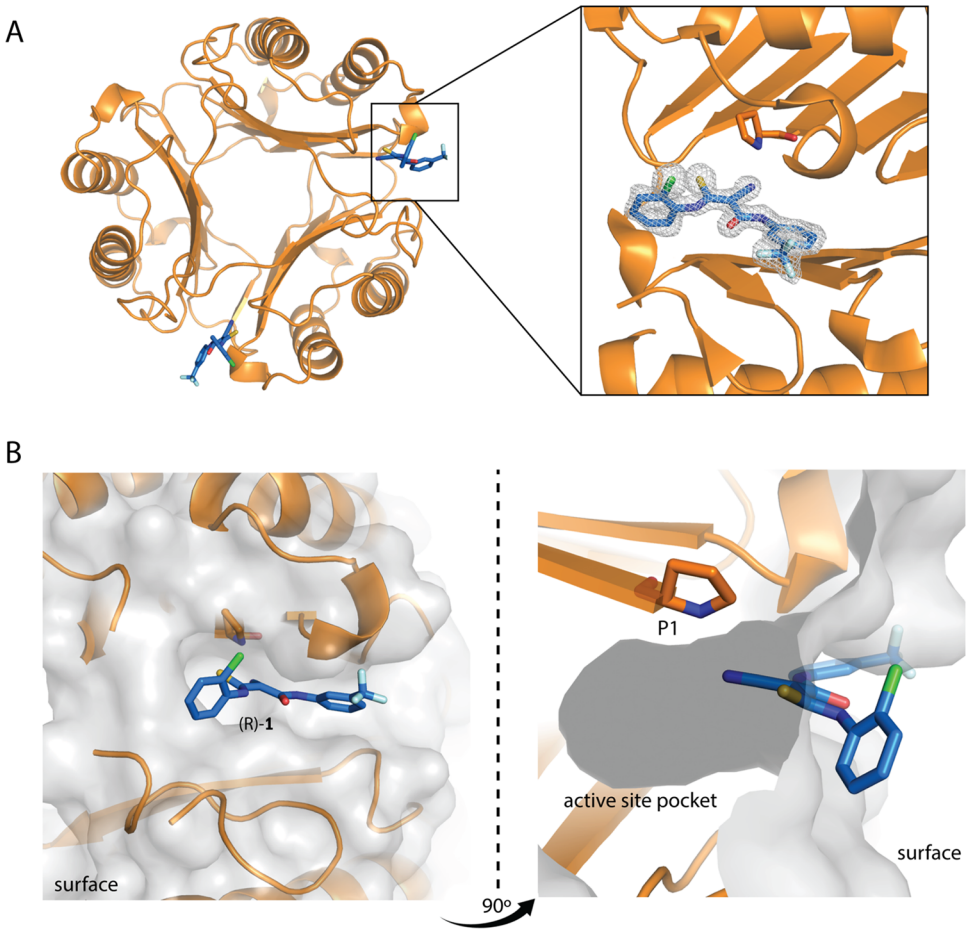

Figure 2. Crystallographic analysis of MIF-1. (A) The 2Fo-Fc electron density map of **1** (gray mesh) was clearly observed in two out of three MIF subunits. The (R)-enantiomer of the inhibitor (blue sticks) binds on the surface of MIF (orange cartoon) blocking the active site pocket. (B) Binding orientation of **1** in relation to the surface (left) and active site pocket (right) of MIF.

enzymatic site is located at each monomer−monomer interface for the MIF homotrimer and uses the N-terminus Pro1 as a catalytic base.[18] Although a *bona fide* substrate has yet to be identified, model substrates such as 4-hydroxyphenylpyruvate (4-HPP) and D-dopachrome have been discovered and used for drug discovery at this site.[17,19−21] Via this approach, inhibitors that are covalent,[22,23] competitive,[20,24,25] or allosteric[26−29] have been identified and utilized in various disease models to understand the functionality of MIF.

The allosteric inhibitors were found at four separate sites and each had significant biological value.[26−29] The allosteric MIF inhibitor (Dekker-6y), which was recently described by Chen and co-workers, interferes with apoptosis-inducing factor (AIF) colocalization to prevent parthanatos.[26] Ibudilast, which

https://doi.org/10.1021/acsomega.4c10969
ACS Omega 2025, 10, 17441−17452

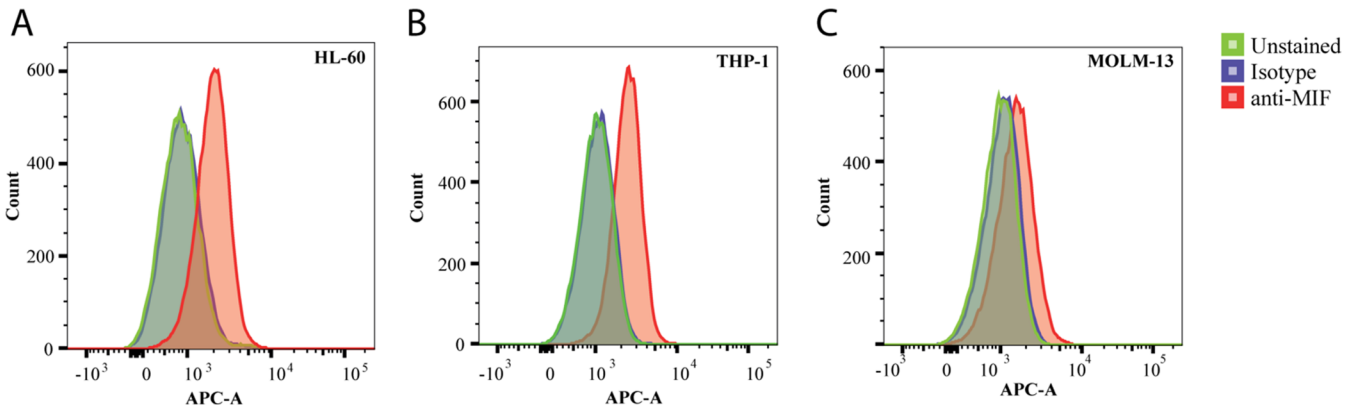

Figure 3. Representative histograms of MIF expression in different AML cell lines. Fixed and permeabilized (A) HL-60, (B) THP-1, or (C) MOLM-13 cells, treated with anti-MIF primary antibody and APC-conjugated secondary antibody, were used to determine the expression levels of MIF (shown in orange). Isotype (purple) and unstained (green) controls are shown for comparison. All experiments were performed in triplicate.

was structurally characterized as an allosteric MIF inhibitor in 2010,[27] is a known anti-inflammatory drug with profound clinical interest especially for multiple sclerosis.[30] Similar to the first two compounds, Chicago Sky Blue 6B (or p425) also binds MIF in an allosteric manner,[28] while its activity was shown to have a neuroprotective and anti-inflammatory effect[31] on brain ischemia. Iguratimod (or T-614) is clinically approved in Japan and China as an antirheumatic drug that binds on the surface of MIF and blocks its active site. Besides the antirheumatic properties, Iguratimod's biological value is also reflected on its protective role against oxidative stress, after acetaminophen overdose.[29,32]

Specifically for the MIF-induced activation of CD74, small molecule modulators of the catalytic activity served a key role in identifying MIF surface residues that regulate activation of the receptor.[22] Interestingly, several other studies have shown that the MIF surface area responsible for activation of CD74 communicates with the backbone dynamics of the catalytic residues Pro1[33] and an allosteric site located at the opening of the solvent channel.[34,35]

Herein, we report the structural and functional characterization of a MIF allosteric inhibitor (compound **1**) that predominantly binds on the protein's surface blocking the active site pocket and the previously reported MIF-CD74 interface. Testing **1** against the NCI-60 cancer cell line panel[36] showed a selective antiproliferative effect of the AML cell line HL-60. Interestingly, HL-60 is known to overexpress MIF.[37,38] Upon further investigation, we confirmed the effect of **1** on HL-60 cells and showed that our finding is applicable to multiple AML cell lines. To obtain mechanistic insights, we interrogated the MIF receptors, CD74, CXCR2, and CXCR4 in the presence of small molecule antagonists or neutralization antibodies. The cell cycle arrest of malignant cells in the G0/G1 phase observed with the inhibition of MIF and CD74, further supports the essential role of the MIF-CD74 axis in the pathogenesis of AML.

RESULTS AND DISCUSSION

Identification and Crystallographic Characterization of a MIF Allosteric Inhibitor. In light of the previously described pathogenic role of MIF in AML, we turned our interest to the identification of a MIF inhibitor with antiproliferation activity against this malignancy. We performed a 96-well high-throughput screen (HTS) with Microsource and Maybridge compound libraries at a single drug dose. The thirty-three compounds identified to inhibit the MIF activity by >90% were selected for downstream characterization using multipoint kinetic assays. 3-(2-chloroanilino)-2-cyano-3-sulfanylidene-*N*-[3-(trifluoromethyl)-phenyl]propanamide (**1**) had emerged as a compound with interesting structural scaffold (Figure 1A) and an inhibition constant (K_i) of 1.3 ± 0.2 μM (Figure 1B).

To exclude the possibility of having an irreversible inhibitor, we also performed second-order kinetics.[22,23] In the case of covalent inhibition, the activity of MIF would drop over time, indicating that a permanent MIF-inhibitor complex is gradually forming and a reduced number of active enzyme molecules are available to catalyze tautomerization of 4-HPP.[39] Our findings demonstrate that the activity of MIF is not significantly altered over the period of 3.5 h, suggesting that the inhibitor binds MIF in a reversible manner (Figure S1). We followed up on enzymatic results and solved the cocrystal structure of MIF-**1** (Figure 2A and Table S1). The 2Fo-Fc electron density map showed an apparent occupancy of **1** on two out of three subunits of MIF. At the same time, the third is partially occupied (Figure 2A).

Structural analysis of the MIF-**1** complex revealed that the (R)-configuration of **1** binds on the surface of MIF, blocking the active site opening (Figure 2B). Our compound binds to the surface of MIF proximal to residues Tyr36, Ile64, Lys66, Trp108, and Asn109 of each subunit (Figure S2), which were previously reported to influence CD74 activation.[22] The inhibitor is stabilized in the active site of MIF by forming one hydrogen bond at 3.0 Å with Tyr95 and several van der Waals interactions with Gln35, Tyr36, Phe49, Ile64, Trp108, and Phe113 (Figure S2). Notably, Phe49 and Tyr95 are derived from the adjacent monomer.

The amino acids involved in the formation of MIF-**1** along with the key stabilization forces applied on the complex suggest that **1** is a selective modulator of MIF. Whereas MIF and its human homologue D-dopachrome tautomerase (D-DT or MIF2) demonstrate low amino acid agreement in their active sites,[40,41] only Ile64 is present in both proteins out of the seven key amino acids reported above. Previous structural studies of MIF2[42−44] showed that protein−ligand complexes are mainly stabilized by hydrogen bonding interactions, something that contradicts with MIF complexes in which hydrophobic interactions are the primary stabilization force.

https://doi.org/10.1021/acsomega.4c10969
ACS Omega 2025, 10, 17441−17452

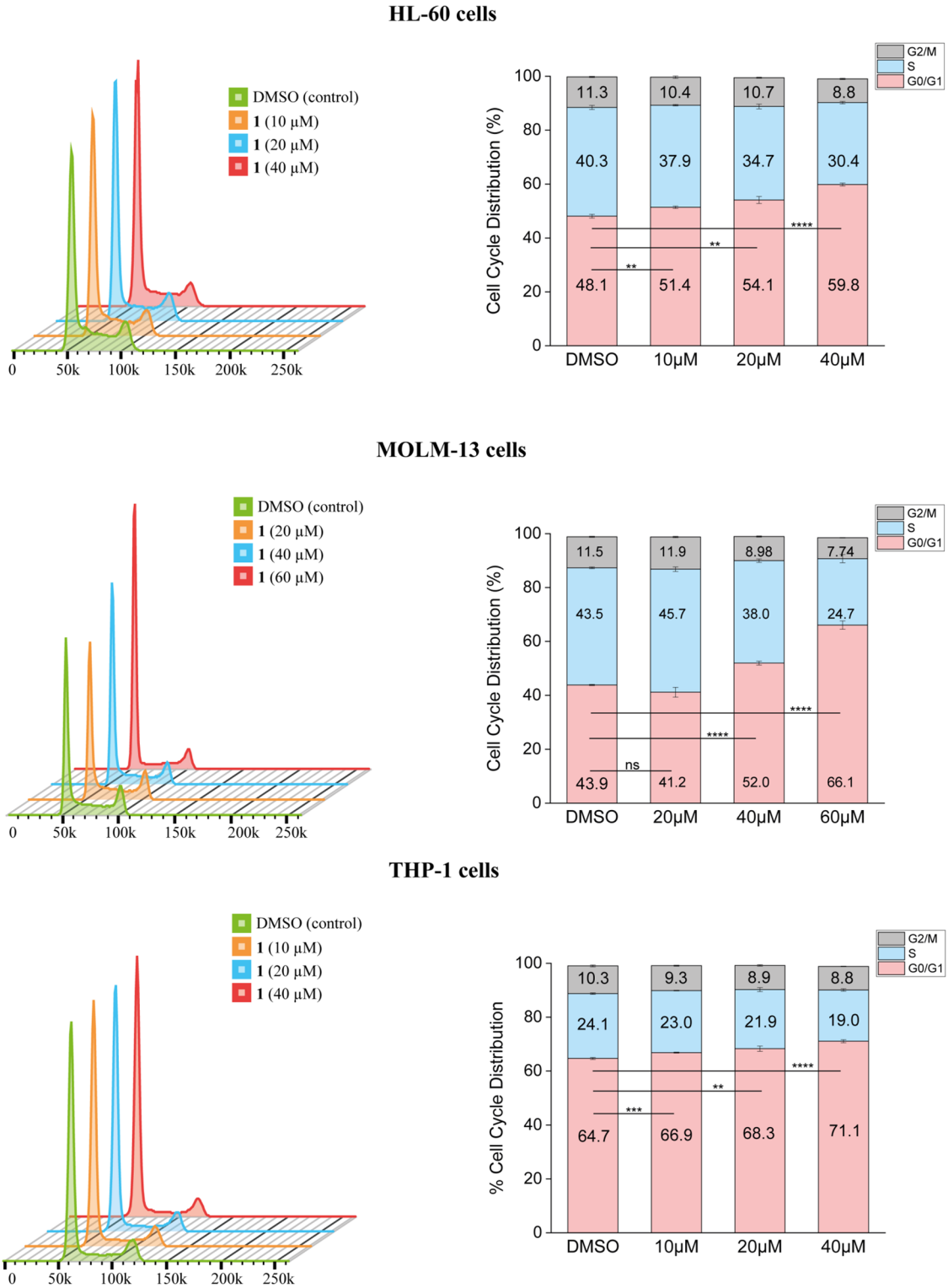

Figure 4. Effect of doses of 1 on the cell cycle of AML cell lines. We examined the impact of compound **1** on the cell cycle of AML cell lines. HL-60, MOLM-13, and THP-1 cells were treated with DMSO (control) and varying concentrations of **1** to analyze the percentages of cells in the G0/G1, S, and G2/M phases through side-by-side experiments. The left side displays representative histograms of propidium iodide fluorescence from the differently treated cells, while the bar graphs on the right illustrate the percentage of cells in each phase of the cell cycle. All experiments were repeated in triplicate and the error is shown as ± SD.

Antitumor Activity and Selectivity of 1 against the NCI-60 Human Tumor Cell Lines. We used the NCI-60 human tumor cell line panel to determine if **1** has an anticancer activity. The molecule was tested at a final concentration of 10 μM and the results were plotted as a percentage of mean proliferative growth (Figure S3). Interestingly, **1** demonstrated selective inhibition activity against HL-60, blocking cell growth by 66%. Since HL-60 is an AML cell line, we also investigated the expression of MIF in two additional AML cell lines, THP-1 and MOLM-13 (Figure 3). All three cell lines express MIF, as

https://doi.org/10.1021/acsomega.4c10969
ACS Omega 2025, 10, 17441−17452

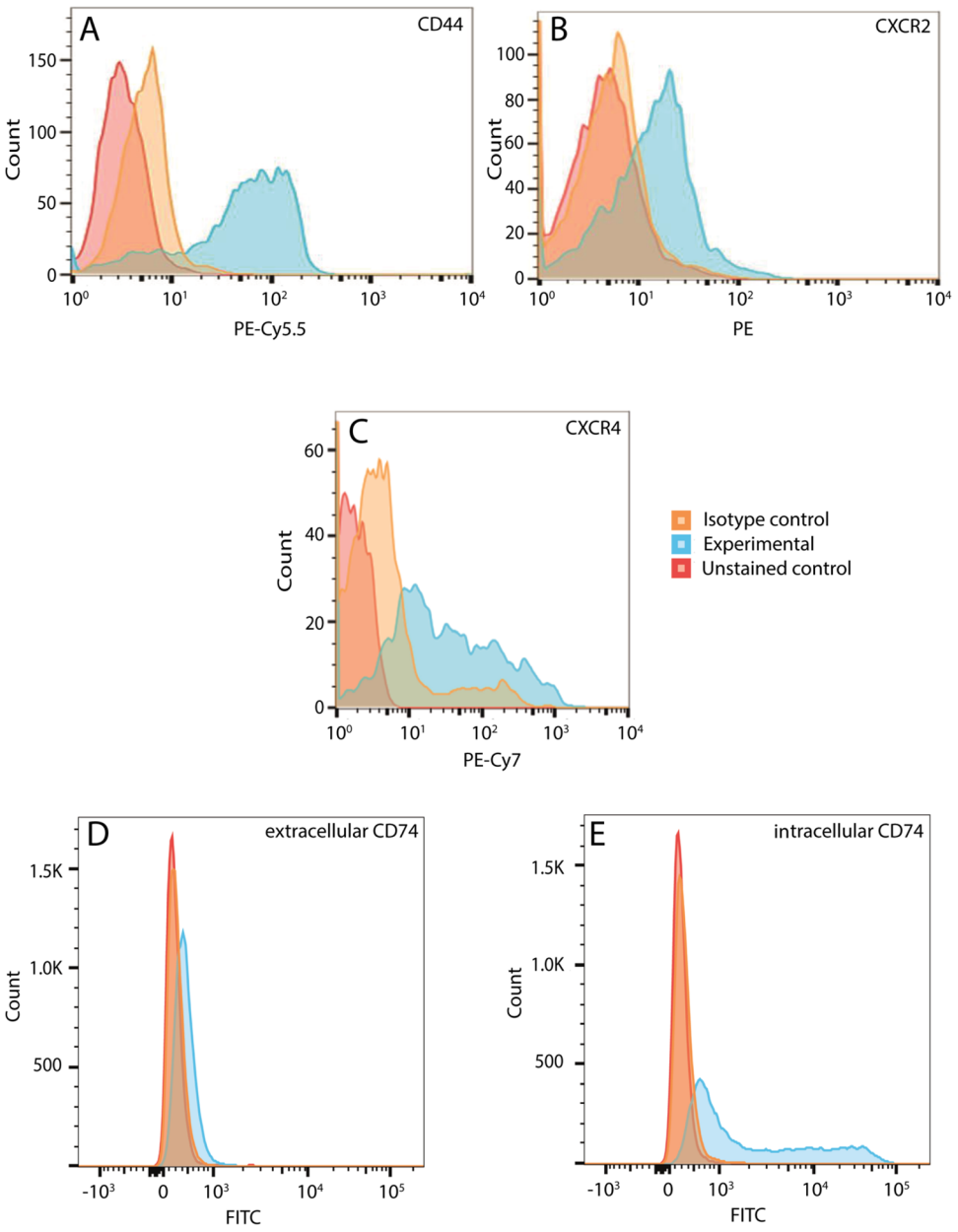

Figure 5. Protein expression analysis of the MIF receptors in HL-60 cells. (A) CD44, (B) CXCR2, (C) CXCR4, (D) extracellular CD74, and (E) intracellular CD74.

shown by the staining in flow cytometry with anti-MIF antibody compared to isotype and unstained controls. HL-60 and THP-1 demonstrate greater expression than MOLM-13.

Effect of 1 on the Cell Cycle and Apoptosis of AML Cells. Studies on MIF-dependent cell proliferation showed effects on the cell cycle and apoptosis, depending on the malignancy.[10,45−48] In this study, both mechanisms were examined. For apoptosis, we utilized the microculture kinetic assay (also called CorrectChemo Assay), a spectrophotometric method measuring changes in the optical properties of cancer cells caused after drug treatments.[49,50] Cell blebbing can be utilized in this case to measure the apoptotic potency of chemotherapeutic agents as compared to control treatments and is reported as kinetic units (KU) of apoptosis. Responses below 1KU correspond to no sensitivity, while responses above 5.8 KU correspond to a high chemosensitivity. Any values in between are considered medium chemosensitivity. **1** was tested at a concentration range of 10 to 200 μM, and the apoptotic responses obtained were compared with the corresponding response of the chemotherapeutic agent topotecan (Figure S4).

Our findings demonstrate apoptotic response with an average KU value of 0.7. This apoptotic response falls into the no-sensitivity region of our assay. From the same experiment, a weak apoptotic response was detected at a starting concentration of 83 μM of **1** (Figure S4). Starting at a concentration of 132 μM, we observed a decline of the optical density (OD) until a plateau was reached. This is a typical curve for cells undergoing necrosis. Collectively, these data show that the mechanism of action of **1** is not related to cell apoptosis.

We next explored the impact of **1** on cell cycle. The AML cell lines, HL-60, MOLM-13, and THP-1 were treated with various concentrations of **1** and the findings were compared

https://doi.org/10.1021/acsomega.4c10969
ACS Omega 2025, 10, 17441−17452

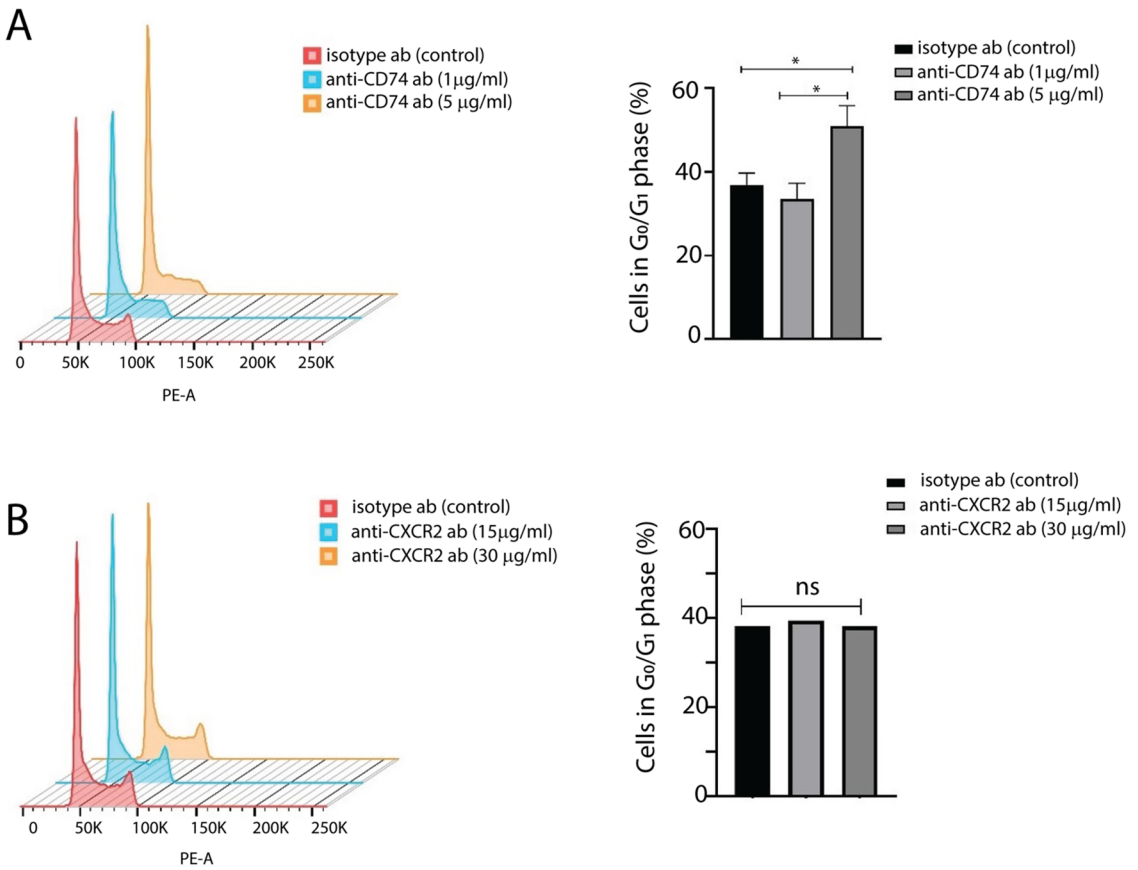

Figure 6. Flow cytometric analysis of the impact of CD74 or CXCR2 inhibition on the cell cycle of HL-60 cells. Cells were treated with different concentrations of neutralizing antibodies to (A) CD74 or (B) CXCR2. Histograms of propidium iodide fluorescence in these cells are displayed on the left and were used to determine the percentage of cells in G0/G1 upon different treatments (right). The percentage of cells in G0/G1 cells are plotted as bar graphs. All experiments were performed in triplicate and the error is shown as ± SD.

with corresponding control treatments. Cell cycle distribution analysis of all three cell lines demonstrated a clear increase in the percentage of cells found in the G0/G1 phase (Figure 4). Arrest in the G0/G1 phase was concentration-dependent in the three cell lines with HL-60 affected the most. In comparison to the control, treatment with 40 μM of **1** led to 11.7% of HL-60, 8.1% of MOLM-13, and 6.4% of THP-1 cell arrest in the G0/G1 phase. In agreement with the MIF expression patterns (Figure 3) and at the lowest shared concentration of 20 μM, HL-60, and THP-1 cells showed a statistically significant percentage of cells arrested in the G0/G1 phase. In contrast, MOLM-13 cells needed higher concentrations of **1** to demonstrate these effects.

Expression of MIF Receptors and Preliminary Evidence of the MIF-1 Pathway of Action. To deepen our understanding into the mechanism of **1**, we investigated the MIF receptors present on the surface of HL-60 cells. According to our analysis, the two chemokine receptors, CXCR2 and CXCR4, and the CD74/CD44 coreceptor pair are present (Figure 5). For CD74, we had to determine both the extracellular and intracellular protein levels, as this receptor is characterized by a fast internalization rate.[51]

Next, we performed cell proliferation assays. In the absence of a small molecule antagonist for CD74, we only utilized the selective CXCR2 (SB225002) and CXCR4 (AMD3100) antagonists to examine whether cell proliferation is dependent on these two receptors. Given its previously identified antiproliferative effect, **1** was used as a control for this experiment. SB225002 and **1** inhibited cell proliferation of HL-60 with half-maximal inhibitory concentration (IC_{50}) values of 32.7 μM and 15.9 μM, respectively, while AMD3100 had no effect (Figure S5). Interestingly, a previous study highlighted the role of CXCR2 in AML stem cell proliferation, but in that case activation of CXCR2 was triggered by interleukin-8 (IL-8) and not MIF.[52]

The three-dimensional structure of MIF-**1** complex (Figures 2 and S2) provided evidence that **1** may potentially interfere with CD74 activation. It had been established that the MIF catalytic pocket is not part of the MIF-CD74 interface, but surface residues surrounding the enzymatic pocket play an important role in the activation of CD74.[22] Specifically, Tyr36, Ile64, and Trp108 are three of the five residues that form van der Waals interaction with **1**, and at the same time are identified to influence activation of CD74. These findings led us to postulate that the functional effect of **1** may be associated with the primary MIF receptor, CD74.

Receptor Selectivity by the MIF-1 Complex. Since CXCR4 inhibition did not have any impact on HL-60 cell proliferation (Figure S5C), it became apparent that cycle arrest of AML cells (Figure 4) is related to either inhibition of CD74 or CXCR2. To identify the affected pathway, we treated HL-60 cells with CD74 or CXCR2 neutralization antibodies and the findings were compared with isotype treatments (Figure 6A,B). For the CD74 experiment, treatment with 5 μg/mL of anti-CD74 antibody caused a significant shift of HL-60 cells in the

https://doi.org/10.1021/acsomega.4c10969
ACS Omega 2025, 10, 17441−17452

G0/G1 phase while the anti-CXCR2 antibody had no effect at either 15 μg/mL or 30 μg/mL.

CONCLUSIONS

Upregulation of MIF has been demonstrated in several human cancers and many small-molecule inhibitors targeting its catalytic site have been used in cells and animal models to investigate the mechanism of action.[53−58] Although there is a clear need for precision medicine to target MIF-mediated cancers, developing an FDA-approved drug is challenging. Localization of MIF in intracellular compartments and the extracellular space, interactions with several soluble and membrane-bound proteins, and participation in multiple signaling pathways are some of the MIF challenges that need to be overcome to develop an effective therapeutic. The exact mechanism of CD74 activation, through which MIF primarily exhibits its pathogenic effects in various cancers, is still not completely understood and remains a significant hurdle in drug development.

Apart from the challenges mentioned above, we should also consider the functional role of MIF2. MIF2 is the second human member of the MIF superfamily that shares the tautomerase,[59] endonuclease,[60] and most notable cytokine activities with MIF.[61] The role of the MIF2-CD74 axis in human pathophysiology is currently under investigation. In cancer, MIF2 also promotes cell proliferation.[62] MIF and MIF2 activate CD74 in synergy for certain cancers, such as pancreatic cancer,[63] nonsmall cell lung carcinoma (NSCLC),[64] and neuroblastoma.[65] The synergistic effects of MIF and MIF2 have been previously shown in several solid tumors, but their cooperative function in hematological cancers, particularly AML, is yet to be studied. Recent findings revealed a highly selective inhibitor of MIF2, 2,5-pyridinedicarboxylic acid, which binds the protein and blocks the MIF2-induced activation of CD74 without any noticeable effect on MIF inhibition.[43] While the MIF and MIF2 shared receptor CD74 is highly expressed in AML, **1** and 2,5-pyridine dicarboxylic acid may be combined to investigate a potential synergistic effect of the two proteins in this hematological malignancy. The combined inhibition of MIF and MIF2 could also have a synergistic effect in other cancers. Such molecules have great value as proof-of-principle agents and may be used in combination with other FDA-approved therapeutics to target other pathways in AML.

To provide an unbiased view, we should also acknowledge some limitations of this work. In the absence of small molecule antagonists for CD74, the conclusions derived by studying MIF-**1** offer an indirect perspective of CD74 activation. Direct analysis of MIF-CD74 interactions by either biochemical or structural approaches is not feasible due to the highly flexible and partially disordered structure of the receptor.[66] Unfortunately, the micromolar potency of **1** makes the compound useful only for mechanistic studies, while further structure−activity relationship (SAR) studies are required for therapeutic purposes. Mechanistic investigations of **1** in primary AML samples and xenograft models along with pharmacokinetic and toxicological studies would add value in understanding the functionality of this molecule. Despite these limitations, this study offers a collection of data that are of great importance for the MIF, medicinal chemistry, and AML communities.

Collectively, we report the identification and in vitro characterization of a MIF inhibitor with an allosteric binding motif. Despite the micromolar inhibition potency, **1** shows the key role of MIF in the AML microenvironment. Our findings offer a new avenue for the development of targeted AML therapeutics with lower cytotoxicity. Whereas AML therapeutic plans have not drastically changed for decades, inhibition of MIF signaling should be considered for developing new-generation therapeutics.

MATERIALS AND METHODS

Reagents and Cell Lines. **1** as racemic mixture (MIF inhibitor), SB225002 (CXCR2 antagonist), and AMD3100 (CXCR4 antagonist) were purchased from Maybridge, Santa Cruz Biotechnology, and Abcam, respectively. 4-HPP was purchased from TCI. The purity of all compounds was ≥95%. The BrdU cell proliferation assay kit (catalog#QIA58) was purchased from Millipore. The HL-60 cell line was purchased from the American Type Culture Collection (ATCC). The THP-1 and MOLM-13 cell lines were a generous gift of Prof. Amit Verma, Albert Einstein College of Medicine, USA. For the protein expression analysis of the MIF receptors, the eBioscience antihuman monoclonal antibodies of CD74 (clone 5−329, catalog#11−0748−42) and CD44 (clone IM7, catalog#45−0441−82) were obtained from ThermoFisher Scientific, while the antihuman monoclonal antibodies of CXCR2 (clone 5E8, catalog# 320705) and CXCR4 (clone 12G5, catalog#306513) were purchased from Biolegend. For the MIF expression experiment, the mouse antihuman MIF monoclonal antibody (clone 12302, catalog#MAB289), mouse F(ab)2 IgG (H + L) APC-conjugated antibody (catalog#F0101B), and mouse IgG1 isotype control (clone 11711, catalog#MAB002) were purchased from R&D systems. The neutralizing antihuman CD74 (clone LN-2, catalog#ab9514) was purchased from Abcam, while the neutralizing antihuman CXCR2 (clone 48311, catalog#MAB331) was purchased from R&D Systems.

Protein Expression and Purification. MIF was expressed and purified as described.[35,67,68] Briefly, the MIF gene was inserted in a pET-11b vector and transformed into *Escherichia coli* BL21-Gold (DE3) cells. For expression, cells were grown at 37 °C to an OD_{600} of 0.6 and induced by adding isopropyl β-D-1-thiogalactopyranoside (IPTG) at a final concentration of 1 mM. After 4 h, the cells were collected by centrifugation and stored at −80 °C. For MIF purification, the cells were resuspended in 20 mM Tris, pH 7.4 with 20 mM NaCl containing a mini, EDTA-free protease inhibitor cocktail tablet (Sigma-Aldrich) and lysed by sonication. Cell lysate was loaded onto Q and SP Sepharose columns connected in series and flow-through contained MIF (∼95% pure). The remaining amount of impurity was removed by size-exclusion chromatography (16/60 Superdex 75) using 20 mM Tris, pH 7.4 with 20 mM NaCl as the running buffer. MIF concentration was determined using the Pierce BCA Protein Assay Kit (Thermo Fisher Scientific).

Crystallization of MIF-1 Complex and Structure Determination. For crystallization of MIF-**1** complex, the protein was concentrated at 18 mg/mL and mixed with the inhibitor at 1:3 molar ratio of MIF:**1**. The mixture was incubated at 4 °C overnight and spun down to remove any precipitation. The MIF-**1** complex was crystallized by vapor diffusion in 24-well hanging drop trays as described before.[22,35] Briefly, the protein-inhibitor complex (**PI**) was mixed with the well solution (**W**) containing 20 mM Tris, pH 7.5, 2 M ammonium sulfate, and 3% 2-propanol at various volume ratios (2 μL **PI**: 2 μL **W**, 3 μL **PI**: 1 μL **W**, and 1 μL **PI**: 3 μL **W**).

https://doi.org/10.1021/acsomega.4c10969
ACS Omega 2025, 10, 17441−17452

The trays were stored at 20 °C and crystals started to form within 2−3 weeks, reaching their maximum size within a month. In each well, the drop volume was 4 μL and the final DMSO concentration was up to 5%. The crystals were flash frozen in mother liquor containing 25−28% glycerol as cryoprotectant and a complete data set was obtained at the Yale School of Medicine Macromolecular Crystallographic Facility using Rigaku Pilatus 200 K Detector with a Rigaku 007 rotating copper anode X-ray generator (wavelength = 1.5418 Å) at a temperature of 100 K. The data set was integrated and scaled using the HKL2000 program suit.[69] The structure of MIF-**1** complex was determined by molecular replacement using PHASER.[70] The crystal structure of wild-type MIF (PDB entry: 3DJH) was used as a search model. The initial model of MIF-**1** was refined by Refmac[71] and COOT.[72] The 2Fo-Fc density of **1** was generated by the CCP4-supported program FFT[73] and visualized with PyMOL.[74] The coordinates (PDB) and crystallographic information file (CIF) of **1**, used for refinement of the MIF-**1** crystal structure, were produced by PRODRG.[75] Ramachandran analysis of the structure showed 0% outliers and 98.8% amino acids in the preferred regions. The detailed statistics of the MIF-**1** structure are shown in Table S1. The structure was deposited in PDB under the accession code 8SON.

Kinetic Assays. The 4-HPP keto/enol tautomerase assay was carried out as described elsewhere.[44,68] Briefly, 4-HPP stock solution (100 mM) was freshly prepared in 50 mM ammonium acetate, pH 6.2. The stock solution was incubated overnight in the dark at room temperature to favor the equilibration of 4-HPP to its keto form. A mixture containing 0.420 M borate, MIF at a final concentration of 100 nM, and the different concentrations of **1** was transferred to a UV transparent flat bottom 96-well plate containing 4-HPP with final concentrations ranging from 0 to 2 mM. Catalytic conversion of the keto to enol form of 4-HPP was evaluated by measuring absorption of the 4-HPP enol-borate complex at 306 nm (ε_{306} = 11,400 M^{-1} cm^{-1}) for a total of 90 s. The second-order kinetics experiment was performed similarly to the procedure described above, following a previously published protocol.[22] All the kinetic experiments were performed in triplicate.

Cell BrdU Proliferation Assay. HL-60 cells were grown in RPMI supplemented with 2 mM glutamine, 10% fetal bovine serum (FBS), and 1% pen/strep until they reached a density of 1 × 10^6 cells/mL. The cells were then centrifuged and resuspended in RPMI supplemented with 2 mM glutamine, 0.5% FBS, and 1% pen/strep. 100 μL of cells were seeded at 1 × 10^5 cells/mL in 96-well plates and the experiment was carried out according to the manufacturer's protocol. Cell proliferation experiments were performed in triplicate.

Apoptosis Assay. CorrectChemo apoptosis assay, also known as microculture kinetic assay (MiCK assay),[76] was used to examine the effect of **1** in HL-60 cells. Briefly, HL-60 cells were plated in a 96-well microplate and incubated with different concentrations of **1** (10−200 μM). Morphological changes that occur in cells as they undergo apoptosis (cell blebbing) were monitored over 48 h using a spectrophotometer. 576 readings of the samples were taken at OD_{600} and plotted against time to get V_{max} values. Apoptosis is reported as kinetic units (KU) and compared to KU values of control (40 μM Topotecan).

Protein Expression Analysis by Fluorescence-Activated Cell Sorting (FACS). For protein expression analysis, cells were centrifuged to remove media, washed, and resuspended in FACS buffer (saline +1% v/v FBS). 0.5 × 10^6 cells were added into individual wells of a 96-well plate and fixed for 30 min on ice. After removal of the fixation buffer by centrifugation, the cell pellet was resuspended in FACS buffer with no antibody (unstained control), isotype antibody (isotype control), or an antibody targeting the protein of interest for 30 min on ice, in the dark. The cells were then washed twice with FACS buffer and resuspended in FACS buffer for analysis on BD LSRII flow cytometer. For expression analysis of intracellular CD74 and MIF, the same procedure as described above was followed except the cells were fixed and permeabilized with BD FIX/PERM buffer. Since MIF has no commercially available fluorophore-conjugated primary antibody, treatment of primary MIF antibody was followed by incubation with Mouse F(ab)2 IgG (H + L) APC-conjugated antibody. All experiments were performed 3 times. Mean fluorescence intensities were computed for unstained, isotype, and antibody-stained samples using FlowJo software, and *t* tests were performed for statistical analysis.

Cell Cycle Analysis. Cell cycle analysis was done as previously described.[77] Briefly, the AML cell lines (HL-60, THP-1, and MOLM-13) were grown in RPMI supplemented with 2 mM glutamine, 10% FBS, and 1% penicillin/streptomycin (pen/strep) until they reached a density of 1 × 10^6 cells/mL. Serum-starved (0.5% FBS) cells were plated in 6-well plates at 1 × 10^6 cells/well, and after overnight incubation, they were treated with DMSO (as control) or varying concentrations of **1**. 24 h after treatment, the cells were harvested for propidium iodide (PI) solution treatment. To determine whether **1** demonstrates its cell cycle arrest effects via upstream inhibition of CXCR2 or CD74, HL-60 cells were plated and serum-starved overnight, as described above. The next day, cells were treated with isotype or different concentrations of neutralizing antibodies for CXCR2 or CD74. 24 h later, the cells were harvested for PI solution staining.

PI Solution Staining and Cell Cycle Arrest Analysis. PI solution staining was done as previously described.[77] Briefly, the harvested cells were centrifuged, and the media was removed. The cells were washed with ice-cold phosphate-buffered saline (PBS). The cells were resuspended in 0.5 mL PBS and fixed with 4.5 mL of 70% ethanol for at least 2 h. After fixation, the cells were centrifuged to remove the ethanol and washed with PBS. After removing PBS, the cell pellet was resuspended in 1 mL of PI staining solution (0.02 mg/mL), Triton X-100 (0.1% v/v), RNase A (0.2 mg/mL) in PBS. The cells were stained for 30 min at room temperature in the dark. After staining, the cells were filtered into tubes compatible with BD LSRII flow cytometer, and the samples were analyzed for PI fluorescence. For analysis, the cell debris and cell doublets were gated out, and the remaining events were analyzed to determine % cells in the different phases of cell cycle for each treatment using FlowJo software.

Statistical Analysis. Statistical analysis between different groups was performed using paired *t* tests in GraphPad Prism 10.0.1.218 (San Diego, CA).

■ ASSOCIATED CONTENT

Data Availability Statement

The crystal structure of MIF-**1** is deposited in PDB (https://www.rcsb.org/) under the accession code 8SON.

https://doi.org/10.1021/acsomega.4c10969
ACS Omega 2025, 10, 17441−17452

Supporting Information

The Supporting Information is available free of charge at https://pubs.acs.org/doi/10.1021/acsomega.4c10969.

Data collection and refinement statistics for MIF-1 (Table S1); second-order kinetic analysis of MIF-1 (Figure S1); crystallographic analysis of MIF-1 interactions (Figure S2); single point screening of 1 against the NCI-60 human tumor cell lines panel (Figure S3); effect of 1 on apoptosis of HL-60 cells (Figure S4), and impact of CXCR2 and CXCR4 inhibition on HL-60 cell proliferation (Figure S5) (PDF)

AUTHOR INFORMATION

Corresponding Authors

Georgios Pantouris − *Department of Chemistry, University of the Pacific, Stockton, California 95211, United States; Department of Pharmacology, School of Medicine, Yale University, New Haven, Connecticut 06510, United States;* orcid.org/0000-0001-5547-1406; Email: gpantouris@pacific.edu

Elias J. Lolis − *Department of Pharmacology, School of Medicine, Yale University, New Haven, Connecticut 06510, United States; Yale Cancer Center, Yale School of Medicine, New Haven, Connecticut 06510, United States;* orcid.org/0000-0002-7902-7868; Email: elias.lolis@yale.edu

Authors

Leepakshi Khurana − *Department of Pharmacology, School of Medicine, Yale University, New Haven, Connecticut 06510, United States*

Pathricia Tilstam − *Department of Internal Medicine, Yale School of Medicine, New Haven, Connecticut 06510, United States*

Alison Benner − *Department of Pharmacology, School of Medicine, Yale University, New Haven, Connecticut 06510, United States*

Thomas Yoonsang Cho − *Department of Pharmacology, School of Medicine, Yale University, New Haven, Connecticut 06510, United States*

Martin Lelaidier − *Diatech Oncology, Montreal, Quebec H3A 0G1, Canada*

Mathieu Perrée − *Diatech Oncology, Montreal, Quebec H3A 0G1, Canada*

Zoe Rosenbaum − *Department of Internal Medicine, Yale School of Medicine, New Haven, Connecticut 06510, United States*

Lin Leng − *Department of Internal Medicine, Yale School of Medicine, New Haven, Connecticut 06510, United States*

Francine Foss − *Hematology and Stem Cell Transplantation, Yale University School of Medicine, New Haven, Connecticut 06510, United States; Yale Cancer Center, Yale School of Medicine, New Haven, Connecticut 06510, United States*

Vineet Bhandari − *Division of Neonatology, Department of Pediatrics, The Children's Regional Hospital at Cooper, Camden, New Jersey 08103, United States*

Amit Verma − *Albert Einstein College of Medicine, Montefiore Medical Center, Bronx, New York 10461, United States*

Richard Bucala − *Department of Internal Medicine, Yale School of Medicine, New Haven, Connecticut 06510, United States; Yale Cancer Center, Yale School of Medicine, New Haven, Connecticut 06510, United States*

Complete contact information is available at: https://pubs.acs.org/10.1021/acsomega.4c10969

Author Contributions

Conceptualization, G.P. and E.L.; methodology, G.P. and L.K.; validation, G.P. and E.L.; formal analysis, G.P., L.K., P.T., M.L., M.P., Z.R., and L.L.; investigation, G.P., L.K., P.T., A.B., T.Y.C., M.L., M.P., and Z.R.; resources, G.P., A.V., R.B., and E.L.; data curation, G.P. and E.L.; writing-original draft preparation, G.P. and L.K.; writing—review and editing, G.P., L.K., V.B., and E.L.; supervision, G.P., L.L., R.B., and E.L.; funding acquisition, G.P., F.F., R.B., and E.L. All authors have read and agreed to the published version of the manuscript.

Notes

This work was prepared while Thomas Yoonsang Cho was employed at Yale University. The opinions expressed in this article are the author's own and do not reflect the view of the National Institutes of Health, the Department of Health and Human Services, or the United States government.

The authors declare no competing financial interest.

ACKNOWLEDGMENTS

This research was funded by Robert E. Leet and Clara Guthrie Patterson Trust Fellowship Program in Clinical Research, Bank of America, N.A., Trustee (G.P.), Schussel gift account (F.F.), the National Institutes of Health Grants AI065029, AI082295 (E.L.), and S10-OD018007−01 (instrumentation grant).

REFERENCES

(1) Khwaja, A.; Bjorkholm, M.; Gale, R. E.; Levine, R. L.; Jordan, C. T.; Ehninger, G.; Bloomfield, C. D.; Estey, E.; Burnett, A.; Cornelissen, J. J.; Scheinberg, D. A.; Bouscary, D.; Linch, D. C. Acute myeloid leukaemia. *Nat. Rev. Dis. Primers* **2016**, *2*, No. 16010.

(2) van Galen, P.; Hovestadt, V.; Wadsworth, M. H., II; Hughes, T. K.; Griffin, G. K.; Battaglia, S.; Verga, J. A.; Stephansky, J.; Pastika, T. J.; Story, J. L.; Pinkus, G. S.; Pozdnyakova, O.; Galinsky, I.; Stone, R. M.; Graubert, T. A.; Shalek, A. K.; Aster, J. C.; Lane, A. A.; Bernstein, B. E. Single-Cell RNA-Seq Reveals AML Hierarchies Relevant to Disease Progression and Immunity. *Cell* **2019**, *176* (6), 1265−1281.e24.

(3) Alaggio, R.; Amador, C.; Anagnostopoulos, I.; Attygalle, A. D.; Araujo, I. B. O.; Berti, E.; Bhagat, G.; Borges, A. M.; Boyer, D.; Calaminici, M.; Chadburn, A.; Chan, J. K. C.; Cheuk, W.; Chng, W. J.; Choi, J. K.; Chuang, S. S.; Coupland, S. E.; Czader, M.; Dave, S. S.; de Jong, D.; Du, M. Q.; Elenitoba-Johnson, K. S.; Ferry, J.; Geyer, J.; Gratzinger, D.; Guitart, J.; Gujral, S.; Harris, M.; Harrison, C. J.; Hartmann, S.; Hochhaus, A.; Jansen, P. M.; Karube, K.; Kempf, W.; Khoury, J.; Kimura, H.; Klapper, W.; Kovach, A. E.; Kumar, S.; Lazar, A. J.; Lazzi, S.; Leoncini, L.; Leung, N.; Leventaki, V.; Li, X. Q.; Lim, M. S.; Liu, W. P.; Louissaint, A., Jr.; Marcogliese, A.; Medeiros, L. J.; Michal, M.; Miranda, R. N.; Mitteldorf, C.; Montes-Moreno, S.; Morice, W.; Nardi, V.; Naresh, K. N.; Natkunam, Y.; Ng, S. B.; Oschlies, I.; Ott, G.; Parrens, M.; Pulitzer, M.; Rajkumar, S. V.; Rawstron, A. C.; Rech, K.; Rosenwald, A.; Said, J.; Sarkozy, C.; Sayed, S.; Saygin, C.; Schuh, A.; Sewell, W.; Siebert, R.; Sohani, A. R.; Tooze, R.; Traverse-Glehen, A.; Vega, F.; Vergier, B.; Wechalekar, A. D.; Wood, B.; Xerri, L.; Xiao, W. The 5th edition of the World Health Organization Classification of Haematolymphoid Tumours: Lymphoid Neoplasms. *Leukemia* **2022**, *36* (7), 1720−1748.

(4) Rai, K. R.; Holland, J. F.; Glidewell, O. J.; Weinberg, V.; Brunner, K.; Obrecht, J. P.; Preisler, H. D.; Nawabi, I. W.; Prager, D.; Carey, R. W.; Cooper, M. R.; Haurani, F.; Hutchison, J. L.; Silver, R. T.; Falkson, G.; Wiernik, P.; Hoagland, H. C.; Bloomfield, C. D.; James, G. W.; Gottlieb, A.; Ramanan, S. V.; Blom, J.; Nissen, N. I.; Bank, A.; Ellison, R. R.; Kung, F.; Henry, P.; McIntyre, O. R.; Kaan, S. K.

Treatment of acute myelocytic leukemia: a study by cancer and leukemia group B. *Blood* **1981**, *58* (6), 1203−1212.
(5) Kantarjian, H.; Kadia, T.; DiNardo, C.; Daver, N.; Borthakur, G.; Jabbour, E.; Garcia-Manero, G.; Konopleva, M.; Ravandi, F. Acute myeloid leukemia: current progress and future directions. *Blood Cancer J.* **2021**, *11* (2), No. 41.
(6) Calandra, T.; Roger, T. Macrophage migration inhibitory factor: a regulator of innate immunity. *Nat. Rev. Immunol.* **2003**, *3* (10), 791−800.
(7) Onodera, S.; Suzuki, K.; Matsuno, T.; Kaneda, K.; Takagi, M.; Nishihira, J. Macrophage migration inhibitory factor induces phagocytosis of foreign particles by macrophages in autocrine and paracrine fashion. *Immunology* **1997**, *92* (1), 131−137.
(8) Barthelmess, R. M.; Stijlemans, B.; Van Ginderachter, J. A. Hallmarks of Cancer Affected by the MIF Cytokine Family. *Cancers* **2023**, *15* (2), No. 395, DOI: 10.3390/cancers15020395.
(9) Abdul-Aziz, A. M.; Shafat, M. S.; Sun, Y.; Marlein, C. R.; Piddock, R. E.; Robinson, S. D.; Edwards, D. R.; Zhou, Z.; Collins, A.; Bowles, K. M.; Rushworth, S. A. HIF1alpha drives chemokine factor pro-tumoral signaling pathways in acute myeloid leukemia. *Oncogene* **2018**, *37* (20), 2676−2686.
(10) Spertini, C.; Bénéchet, A. P.; Birch, F.; Bellotti, A.; Román-Trufero, M.; Arber, C.; Auner, H. W.; Mitchell, R. A.; Spertini, O.; Smirnova, T. Macrophage migration inhibitory factor blockade reprograms macrophages and disrupts prosurvival signaling in acute myeloid leukemia. *Cell Death Discovery* **2024**, *10* (1), No. 157.
(11) Shi, X.; Leng, L.; Wang, T.; Wang, W.; Du, X.; Li, J.; McDonald, C.; Chen, Z.; Murphy, J. W.; Lolis, E.; Noble, P.; Knudson, W.; Bucala, R. CD44 is the signaling component of the macrophage migration inhibitory factor-CD74 receptor complex. *Immunity* **2006**, *25* (4), 595−606.
(12) Jin, L.; Hope, K. J.; Zhai, Q.; Smadja-Joffe, F.; Dick, J. E. Targeting of CD44 eradicates human acute myeloid leukemic stem cells. *Nat. Med.* **2006**, *12* (10), 1167−1174.
(13) Yu, X.; Munoz-Sagredo, L.; Streule, K.; Muschong, P.; Bayer, E.; Walter, R. J.; Gutjahr, J. C.; Greil, R.; Concha, M. L.; Müller-Tidow, C.; Hartmann, T. N.; Orian-Rousseau, V. CD44 loss of function sensitizes AML cells to the BCL-2 inhibitor venetoclax by decreasing CXCL12-driven survival cues. *Blood* **2021**, *138* (12), 1067−1080.
(14) Ruvolo, P. P.; Hu, C. W.; Qiu, Y.; Ruvolo, V. R.; Go, R. L.; Hubner, S. E.; Coombes, K. R.; Andreeff, M.; Qutub, A. A.; Kornblau, S. M. LGALS3 is connected to CD74 in a previously unknown protein network that is associated with poor survival in patients with AML. *eBioMedicine* **2019**, *44*, 126−137.
(15) Bernhagen, J.; Krohn, R.; Lue, H.; Gregory, J. L.; Zernecke, A.; Koenen, R. R.; Dewor, M.; Georgiev, I.; Schober, A.; Leng, L.; Kooistra, T.; Fingerle-Rowson, G.; Ghezzi, P.; Kleemann, R.; McColl, S. R.; Bucala, R.; Hickey, M. J.; Weber, C. MIF is a noncognate ligand of CXC chemokine receptors in inflammatory and atherogenic cell recruitment. *Nat. Med.* **2007**, *13* (5), 587−596.
(16) Wang, Y.; An, R.; Umanah, G. K.; Park, H.; Nambiar, K.; Eacker, S. M.; Kim, B.; Bao, L.; Harraz, M. M.; Chang, C.; Chen, R.; Wang, J. E.; Kam, T. I.; Jeong, J. S.; Xie, Z.; Neifert, S.; Qian, J.; Andrabi, S. A.; Blackshaw, S.; Zhu, H.; Song, H.; Ming, G. L.; Dawson, V. L.; Dawson, T. M. A nuclease that mediates cell death induced by DNA damage and poly(ADP-ribose) polymerase-1. *Science* **2016**, *354* (6308), No. aad6872, DOI: 10.1126/science.aad6872.
(17) Rosengren, E.; Aman, P.; Thelin, S.; Hansson, C.; Ahlfors, S.; Bjork, P.; Jacobsson, L.; Rorsman, H. The macrophage migration inhibitory factor MIF is a phenylpyruvate tautomerase. *FEBS Lett.* **1997**, *417* (1), 85−88.
(18) Sun, H. W.; Bernhagen, J.; Bucala, R.; Lolis, E. Crystal structure at 2.6-A resolution of human macrophage migration inhibitory factor. *Proc. Natl. Acad. Sci. U.S.A.* **1996**, *93* (11), 5191−5196.
(19) Rosengren, E.; Bucala, R.; Aman, P.; Jacobsson, L.; Odh, G.; Metz, C. N.; Rorsman, H. The immunoregulatory mediator macrophage migration inhibitory factor (MIF) catalyzes a tautomerization reaction. *Mol. Med.* **1996**, *2* (1), 143−149.
(20) Lubetsky, J. B.; Dios, A.; Han, J.; Aljabari, B.; Ruzsicska, B.; Mitchell, R.; Lolis, E.; Al-Abed, Y. The tautomerase active site of macrophage migration inhibitory factor is a potential target for discovery of novel anti-inflammatory agents. *J. Biol. Chem.* **2002**, *277* (28), 24976−24982.
(21) Parkins, A.; Sandin, S. I.; Knittel, J.; Franz, A. H.; Ren, J.; de Alba, E.; Pantouris, G. Underrepresented Impurities in 4-Hydroxyphenylpyruvate Affect the Catalytic Activity of Multiple Enzymes. *Anal. Chem.* **2023**, *95* (11), 4957−4965.
(22) Pantouris, G.; Syed, M. A.; Fan, C.; Rajasekaran, D.; Cho, T. Y.; Rosenberg, E. M., Jr.; Bucala, R.; Bhandari, V.; Lolis, E. J. An Analysis of MIF Structural Features that Control Functional Activation of CD74. *Chem. Biol.* **2015**, *22* (9), 1197−1205.
(23) Singh, A. K.; Pantouris, G.; Borosch, S.; Rojanasthien, S.; Cho, T. Y. Structural basis for decreased induction of class IB PI3-kinases expression by MIF inhibitors. *J. Cell Mol. Med.* **2017**, *21* (1), 142−153.
(24) Xiao, Z.; Chen, D.; Song, S.; van der Vlag, R.; van der Wouden, P. E.; van Merkerk, R.; Cool, R. H.; Hirsch, A. K. H.; Melgert, B. N.; Quax, W. J.; Poelarends, G. J.; Dekker, F. J. 7-Hydroxycoumarins Are Affinity-Based Fluorescent Probes for Competitive Binding Studies of Macrophage Migration Inhibitory Factor. *J. Med. Chem.* **2020**, *63* (20), 11920−11933.
(25) Cournia, Z.; Leng, L.; Gandavadi, S.; Du, X.; Bucala, R.; Jorgensen, W. L. Discovery of human macrophage migration inhibitory factor (MIF)-CD74 antagonists via virtual screening. *J. Med. Chem.* **2009**, *52* (2), 416−424.
(26) Chen, D.; Osipyan, A.; Adriana, J.; Kader, M.; Gureev, M.; Knol, C. W. J.; Sigmund, M. C.; Xiao, Z.; van der Wouden, P. E.; Cool, R. H.; Poelarends, G. J.; Dekker, F. J. Allosteric Inhibitors of Macrophage Migration Inhibitory Factor (MIF) Interfere with Apoptosis-Inducing Factor (AIF) Co-Localization to Prevent Parthanatos. *J. Med. Chem.* **2023**, *66* (13), 8767−8781.
(27) Cho, Y.; Crichlow, G. V.; Vermeire, J. J.; Leng, L.; Du, X.; Hodsdon, M. E.; Bucala, R.; Cappello, M.; Gross, M.; Gaeta, F.; Johnson, K.; Lolis, E. J. Allosteric inhibition of macrophage migration inhibitory factor revealed by ibudilast. *Proc. Natl. Acad. Sci. U.S.A.* **2010**, *107* (25), 11313−11318.
(28) Bai, F.; Asojo, O. A.; Cirillo, P.; Ciustea, M.; Ledizet, M.; Aristoff, P. A.; Leng, L.; Koski, R. A.; Powell, T. J.; Bucala, R.; Anthony, K. G. A novel allosteric inhibitor of macrophage migration inhibitory factor (MIF). *J. Biol. Chem.* **2012**, *287* (36), 30653−30663.
(29) Bloom, J.; Pantouris, G.; He, M.; Aljabari, B.; Mishra, L.; Manjula, R.; Parkins, A.; Lolis, E. J.; Al-Abed, Y. Iguratimod, an allosteric inhibitor of macrophage migration inhibitory factor (MIF), prevents mortality and oxidative stress in a murine model of acetaminophen overdose. *Mol. Med.* **2024**, *30* (1), No. 43.
(30) Fox, R. J.; Coffey, C. S.; Conwit, R.; Cudkowicz, M. E.; Gleason, T.; Goodman, A.; Klawiter, E. C.; Matsuda, K.; McGovern, M.; Naismith, R. T.; Ashokkumar, A.; Barnes, J.; Ecklund, D.; Klingner, E.; Koepp, M.; Long, J. D.; Natarajan, S.; Thornell, B.; Yankey, J.; Bermel, R. A.; Debbins, J. P.; Huang, X.; Jagodnik, P.; Lowe, M. J.; Nakamura, K.; Narayanan, S.; Sakaie, K. E.; Thoomukuntla, B.; Zhou, X.; Krieger, S.; Alvarez, E.; Apperson, M.; Bashir, K.; Cohen, B. A.; Coyle, P. K.; Delgado, S.; Dewitt, L. D.; Flores, A.; Giesser, B. S.; Goldman, M. D.; Jubelt, B.; Lava, N.; Lynch, S. G.; Moses, H.; Ontaneda, D.; Perumal, J. S.; Racke, M.; Repovic, P.; Riley, C. S.; Severson, C.; Shinnar, S.; Suski, V.; Weinstock-Guttman, B.; Yadav, V.; Zabeti, A. Phase 2 Trial of Ibudilast in Progressive Multiple Sclerosis. *N. Engl. J. Med.* **2018**, *379* (9), 846−855.
(31) Pomierny, B.; Krzyżanowska, W.; Skórkowska, A.; Jurczyk, J.; Budziszewska, B.; Pera, J. Chicago sky blue 6B exerts neuroprotective and anti-inflammatory effects on focal cerebral ischemia. *Biomed. Pharmacother* **2024**, *170*, No. 116102.
(32) Bloom, J.; Metz, C.; Nalawade, S.; Casabar, J.; Cheng, K. F.; He, M.; Sherry, B.; Coleman, T.; Forsthuber, T.; Al-Abed, Y.

Identification of Iguratimod as an Inhibitor of Macrophage Migration Inhibitory Factor (MIF) with Steroid-sparing Potential. *J. Biol. Chem.* **2016**, *291* (51), 26502−26514.
(33) Parkins, A.; Skeens, E.; McCallum, C. M.; Lisi, G. P.; Pantouris, G. The N-terminus of MIF regulates the dynamic profile of residues involved in CD74 activation. *Biophys. J.* **2021**, *120* (18), 3893−3900.
(34) Skeens, E.; Pantouris, G.; Shah, D.; Manjula, R.; Ombrello, M. J.; Maluf, N. K.; Bhandari, V.; Lisi, G. P.; Lolis, E. J. A Cysteine Variant at an Allosteric Site Alters MIF Dynamics and Biological Function in Homo- and Heterotrimeric Assemblies. *Front. Mol. Biosci.* **2022**, *9*, No. 783669.
(35) Pantouris, G.; Ho, J.; Shah, D.; Syed, M. A.; Leng, L.; Bhandari, V.; Bucala, R.; Batista, V. S.; Loria, J. P.; Lolis, E. J. Nanosecond Dynamics Regulate the MIF-Induced Activity of CD74. *Angew. Chem., Int. Ed.* **2018**, *57* (24), 7116−7119.
(36) Shoemaker, R. H. The NCI60 human tumour cell line anticancer drug screen. *Nat. Rev. Cancer* **2006**, *6* (10), 813−823.
(37) Georgouli, M.; Papadimitriou, L.; Glymenaki, M.; Patsaki, V.; Athanassakis, I. Expression of MIF and CD74 in leukemic cell lines: correlation to DR expression destiny. *Biol. Chem.* **2016**, *397* (6), 519−528.
(38) Nishihira, J.; Koyama, Y.; Mizue, Y. Identification of macrophage migration inhibitory factor in human leukemia HL-60 cells and its induction by lipopolysaccharide. *IUBMB Life* **1996**, *40* (5), 861−869.
(39) Crichlow, G. V.; Fan, C.; Keeler, C.; Hodsdon, M.; Lolis, E. J. Structural interactions dictate the kinetics of macrophage migration inhibitory factor inhibition by different cancer-preventive isothiocyanates. *Biochemistry* **2012**, *51* (38), 7506−7514.
(40) Rajasekaran, D.; Zierow, S.; Syed, M.; Bucala, R.; Bhandari, V.; Lolis, E. J. Targeting distinct tautomerase sites of D-DT and MIF with a single molecule for inhibition of neutrophil lung recruitment. *FASEB J.* **2014**, *28* (11), 4961−4971.
(41) Chen, E.; Reiss, K.; Shah, D.; Manjula, R.; Allen, B.; Murphy, E. L.; Murphy, J. W.; Batista, V. S.; Bhandari, V.; Lolis, E. J.; Lisi, G. P. A structurally preserved allosteric site in the MIF superfamily affects enzymatic activity and CD74 activation in D-dopachrome tautomerase. *J. Biol. Chem.* **2021**, *297* (3), No. 101061.
(42) Parkins, A.; Pilien, A. V. R.; Wolff, A. M.; Argueta, C.; Vargas, J.; Sadeghi, S.; Franz, A. H.; Thompson, M. C.; Pantouris, G. The C-terminal Region of D-DT Regulates Molecular Recognition for Protein-Ligand Complexes. *J. Med. Chem.* **2024**, *67* (9), 7359−7372.
(43) Parkins, A.; Das, P.; Prahaladan, V.; Rangel, V. M.; Xue, L.; Sankaran, B.; Bhandari, V.; Pantouris, G. 2,5-Pyridinedicarboxylic acid is a bioactive and highly selective inhibitor of D-dopachrome tautomerase. *Structure* **2023**, *31* (3), 355−367.e4.
(44) Pantouris, G.; Bucala, R.; Lolis, E. J. Structural Plasticity in the C-Terminal Region of Macrophage Migration Inhibitory Factor-2 Is Associated with an Induced Fit Mechanism for a Selective Inhibitor. *Biochemistry* **2018**, *57* (26), 3599−3605.
(45) Utispan, K.; Koontongkaew, S. Macrophage migration inhibitory factor modulates proliferation, cell cycle, and apoptotic activity in head and neck cancer cell lines. *J. Dent. Sci.* **2021**, *16* (1), 342−348.
(46) Xiao, Z.; Song, S.; Chen, D.; van Merkerk, R.; van der Wouden, P. E.; Cool, R. H.; Quax, W. J.; Poelarends, G. J.; Melgert, B. N.; Dekker, F. J. Proteolysis Targeting Chimera (PROTAC) for Macrophage Migration Inhibitory Factor (MIF) Has Anti-Proliferative Activity in Lung Cancer Cells. *Angew. Chem., Int. Ed.* **2021**, *60* (32), 17514−17521.
(47) Denz, A.; Pilarsky, C.; Muth, D.; Ruckert, F.; Saeger, H. D.; Grutzmann, R. Inhibition of MIF leads to cell cycle arrest and apoptosis in pancreatic cancer cells. *J. Surg. Res.* **2010**, *160* (1), 29−34.
(48) Li, G. Q.; Xie, J.; Lei, X. Y.; Zhang, L. Macrophage migration inhibitory factor regulates proliferation of gastric cancer cells via the PI3K/Akt pathway. *World J. Gastroenterol* **2009**, *15* (44), 5541−5548.
(49) Kravtsov, V. D.; Greer, J. P.; Whitlock, J. A.; Koury, M. J. Use of the microculture kinetic assay of apoptosis to determine chemosensitivities of leukemias. *Blood* **1998**, *92* (3), 968−980.
(50) Strickland, S. A.; Raptis, A.; Hallquist, A.; Rutledge, J.; Chernick, M.; Perree, M.; Talbott, M. S.; Presant, C. A. Correlation of the microculture-kinetic drug-induced apoptosis assay with patient outcomes in initial treatment of adult acute myelocytic leukemia. *Leuk. Lymphoma* **2013**, *54* (3), 528−534.
(51) Ong, G. L.; Goldenberg, D. M.; Hansen, H. J.; Mattes, M. J. Cell surface expression and metabolism of major histocompatibility complex class II invariant chain (CD74) by diverse cell lines. *Immunology* **1999**, *98* (2), 296−302.
(52) Schinke, C.; Giricz, O.; Li, W.; Shastri, A.; Gordon, S.; Barreyro, L.; Bhagat, T.; Bhattacharyya, S.; Ramachandra, N.; Bartenstein, M.; Pellagatti, A.; Boultwood, J.; Wickrema, A.; Yu, Y.; Will, B.; Wei, S.; Steidl, U.; Verma, A. IL8-CXCR2 pathway inhibition as a therapeutic strategy against MDS and AML stem cells. *Blood* **2015**, *125* (20), 3144−3152.
(53) O'Reilly, C.; Doroudian, M.; Mawhinney, L.; Donnelly, S. C. Targeting MIF in Cancer: Therapeutic Strategies, Current Developments, and Future Opportunities. *Med. Res. Rev.* **2016**, *36* (3), 440−460.
(54) Ioannou, K.; Cheng, K. F.; Crichlow, G. V.; Birmpilis, A. I.; Lolis, E. J.; Tsitsilonis, O. E.; Al-Abed, Y. ISO-66, a novel inhibitor of macrophage migration, shows efficacy in melanoma and colon cancer models. *Int. J. Oncol.* **2014**, *45* (4), 1457−1468.
(55) Lee, S. H.; Kwon, H. J.; Park, S.; Kim, C. I.; Ryu, H.; Kim, S. S.; Park, J. B.; Kwon, J. T. Macrophage migration inhibitory factor (MIF) inhibitor 4-IPP downregulates stemness phenotype and mesenchymal trans-differentiation after irradiation in glioblastoma multiforme. *PLoS One* **2021**, *16* (9), No. e0257375.
(56) Varinelli, L.; Caccia, D.; Volpi, C. C.; Caccia, C.; De Bortoli, M.; Taverna, E.; Gualeni, A. V.; Leoni, V.; Gloghini, A.; Manenti, G.; Bongarzone, I. 4-IPP, a selective MIF inhibitor, causes mitotic catastrophe in thyroid carcinomas. *Endocr.-Relat. Cancer* **2015**, *22* (5), 759−775.
(57) Cheng, B.; Wang, Q.; Song, Y.; Liu, Y.; Liu, Y.; Yang, S.; Li, D.; Zhang, Y.; Zhu, C. MIF inhibitor, ISO-1, attenuates human pancreatic cancer cell proliferation, migration and invasion in vitro, and suppresses xenograft tumour growth in vivo. *Sci. Rep.* **2020**, *10* (1), No. 6741.
(58) Guda, M. R.; Rashid, M. A.; Asuthkar, S.; Jalasutram, A.; Caniglia, J. L.; Tsung, A. J.; Velpula, K. K. Pleiotropic role of macrophage migration inhibitory factor in cancer. *Am. J. Cancer Res.* **2019**, *9* (12), 2760−2773.
(59) Nishihira, J.; Fujinaga, M.; Kuriyama, T.; Suzuki, M.; Sugimoto, H.; Nakagawa, A.; Tanaka, I.; Sakai, M. Molecular cloning of human D-dopachrome tautomerase cDNA: N-terminal proline is essential for enzyme activation. *Biochem. Biophys. Res. Commun.* **1998**, *243* (2), 538−544.
(60) Xiao, Z.; Chen, D.; Mulder, F.; Song, S.; van der Wouden, P. E.; Cool, R. H.; Melgert, B. N.; Poelarends, G. J.; Dekker, F. J. 4-Iodopyrimidine Labeling Reveals Nuclear Translocation and Nuclease Activity for Both MIF and MIF2. *Chem. - Eur. J.* **2022**, *28* (1), No. e202103030.
(61) Merk, M.; Zierow, S.; Leng, L.; Das, R.; Du, X.; Schulte, W.; Fan, J.; Lue, H.; Chen, Y.; Xiong, H.; Chagnon, F.; Bernhagen, J.; Lolis, E.; Mor, G.; Lesur, O.; Bucala, R. The D-dopachrome tautomerase (DDT) gene product is a cytokine and functional homolog of macrophage migration inhibitory factor (MIF). *Proc. Natl. Acad. Sci. U.S.A.* **2011**, *108* (34), E577−E585.
(62) Xiao, Z.; Osipyan, A.; Song, S.; Chen, D.; Schut, R. A.; van Merkerk, R.; van der Wouden, P. E.; Cool, R. H.; Quax, W. J.; Melgert, B. N.; Poelarends, G. J.; Dekker, F. J. Thieno[2,3-d]pyrimidine-2,4(1H,3H)-dione Derivative Inhibits d-Dopachrome Tautomerase Activity and Suppresses the Proliferation of Non-Small Cell Lung Cancer Cells. *J. Med. Chem.* **2022**, *65* (3), 2059−2077.
(63) Guo, D.; Guo, J.; Yao, J.; Jiang, K.; Hu, J.; Wang, B.; Liu, H.; Lin, L.; Sun, W.; Jiang, X. D-dopachrome tautomerase is over-

https://doi.org/10.1021/acsomega.4c10969
ACS Omega 2025, 10, 17441−17452

expressed in pancreatic ductal adenocarcinoma and acts cooperatively with macrophage migration inhibitory factor to promote cancer growth. *Int. J. Cancer* **2016**, *139* (9), 2056−2067.
(64) Coleman, A. M.; Rendon, B. E.; Zhao, M.; Qian, M. W.; Bucala, R.; Xin, D.; Mitchell, R. A. Cooperative regulation of non-small cell lung carcinoma angiogenic potential by macrophage migration inhibitory factor and its homolog, D-dopachrome tautomerase. *J. Immunol.* **2008**, *181* (4), 2330−2337.
(65) Cavalli, E.; Mazzon, E.; Mammana, S.; Basile, M. S.; Lombardo, S. D.; Mangano, K.; Bramanti, P.; Nicoletti, F.; Fagone, P.; Petralia, M. C. Overexpression of Macrophage Migration Inhibitory Factor and Its Homologue D-Dopachrome Tautomerase as Negative Prognostic Factor in Neuroblastoma. *Brain Sci.* **2019**, *9* (10), No. 284, DOI: 10.3390/brainsci9100284.
(66) Jasanoff, A.; Wagner, G.; Wiley, D. C. Structure of a trimeric domain of the MHC class II-associated chaperonin and targeting protein Ii. *EMBO J.* **1998**, *17* (23), 6812−6818.
(67) Pantouris, G.; Rajasekaran, D.; Garcia, A. B.; Ruiz, V. G.; Leng, L.; Jorgensen, W. L.; Bucala, R.; Lolis, E. J. Crystallographic and receptor binding characterization of Plasmodium falciparum macrophage migration inhibitory factor complexed to two potent inhibitors. *J. Med. Chem.* **2014**, *57* (20), 8652−8656.
(68) Parkins, A.; Pantouris, G. Protocol for purification and enzymatic characterization of members of the human macrophage migration inhibitory factor superfamily. *STAR Protoc.* **2023**, *4* (3), No. 102375.
(69) Otwinowski, Z.; Minor, W. Processing of X-ray Diffraction Data Collected in Oscillation Mode. In *Methods in Enzymology*; Elsevier, 1997; Vol. *276*, pp 307−326.
(70) McCoy, A. J.; Grosse-Kunstleve, R. W.; Adams, P. D.; Winn, M. D.; Storoni, L. C.; Read, R. J. Phaser crystallographic software. *J. Appl. Crystallogr.* **2007**, *40* (Pt 4), 658−674.
(71) Winn, M. D.; Murshudov, G. N.; Papiz, M. Z. Macromolecular TLS Refinement in REFMAC at Moderate Resolutions. In *Methods in Enzymology*; Elsevier, 2003; Vol. *374*, pp 300−321.
(72) Emsley, P.; Lohkamp, B.; Scott, W. G.; Cowtan, K. Features and development of Coot. *Acta Crystallogr., Sect. D: Biol. Crystallogr.* **2010**, *66* (Pt 4), 486−501.
(73) Murshudov, G. N.; Vagin, A. A.; Lebedev, A.; Wilson, K. S.; Dodson, E. J. Efficient anisotropic refinement of macromolecular structures using FFT. *Acta Crystallogr., Sect. D: Biol. Crystallogr.* **1999**, *55* (Pt 1), 247−255.
(74) DeLano, W. L. *The PyMOL Molecular Graphics System*; DeLano Scientific: Palo Alto, CA, 2002.
(75) Schüttelkopf, A. W.; van Aalten, D. M. PRODRG: a tool for high-throughput crystallography of protein-ligand complexes. *Acta Crystallogr., Sect. D: Biol. Crystallogr.* **2004**, *60* (Pt 8), 1355−1363.
(76) Kravtsov, V. D. A novel microculture kinetic assay (MiCK assay) for malignant cell growth and chemosensitivity. *Eur. J. Cancer* **1994**, *30* (10), 1564−1570.
(77) Khurana, L.; ElGindi, M.; Tilstam, P. V.; Pantouris, G. Elucidating the Role of an Immunomodulatory Protein in Cancer: From Protein Expression to Functional Characterization. In *Methods in Enzymology*; Elsevier, 2019; Vol. *629*, pp 307−360.

https://doi.org/10.1021/acsomega.4c10969
ACS Omega 2025, 10, 17441−17452